25 to 1044 MeV Protons Scattering from ^{40}Ca

M. S. Uddin[1, 3*], A. U. Huda[1], D. R. Sarker[1] and M. A. Rahman[2]

[1]*Department of Physics, Jagannath University, Dhaka -1100*
[2]*Department of Physics, University of Dhaka, Dhaka – 1000*
[3]*German University Bangladesh, Gazipur -1702*

Abstract

The experimental data for the angular distribution of 25 - 1044 MeV protons elastically scattered from ^{40}Ca have been analyzed in terms of the three parameters formalism of Strong Absorption Model (SAM) of Frahn and Venter. The best fit parameters T, Δ, and μ are obtained. The inelastic scattering of protons from ^{40}Ca leading to the 2^+ and 3^- states are studied to check the validity of the derived elastic scattering parameters. The quadruple and octupole deformation parameters β_2 and β_3 are extracted from the analyses. The deformation parameters are in good agreement with other works.

Keywords: Nuclear reactions and scattering, strong absorption model, elastic and inelastic proton scattering

1. Introduction

Proton-nucleus scattering has been the subject of a number of studies mostly using the optical model. The strong absorption model (SAM) was introduced by Frahn and Venter [1, 2] as an alternate to the optical model, where the projectiles are strongly absorbed by the target nucleus. In these cases the elastic scattering is describable without any knowledge of the absorption mechanism. The nuclear projectiles n, p, ^{3,4}He and heavy ion are strongly absorbed by the target nucleus. The diffraction model or the so-called strong absorption model starts with the direct parameterization of the scattering function η_ℓ [3, 4] avoiding the usual potential concept. Different non-elastic processes are accounted for by making η_ℓ complex. The SAM is particularly suitable to a situation dominated by strong absorption of incident particles at the nuclear surface.

In the present work we study the elastic scattering of protons from ^{40}Ca at 25 – 1044 MeV energies. Angular distribution data for the inelastic scattering of protons leading to 2^+ and 3^- states were then studied using the best fit SAM elastic scattering parameters and the corresponding deformation parameters are extracted.

2. Materials and Method

The strong absorption model (SAM) is used for the theoretical calculation of the differential cross section. The model starts with an explicit functional form for the scattering function η_ℓ as given by

$$\eta_\ell \exp(2i\sigma_\ell) = g(\ell) + i\mu \frac{dg(\ell)}{d\ell} \tag{1}$$

Where, σ_ℓ is the coulomb phase shift for the ℓ-th partial wave and g (ℓ) is a continuous monotonic function of the angular momentum. We consider the Woods - Saxon form of g (ℓ), namely

$$g(\ell) = \left[1 + \exp(T-\ell)\big/\Delta\right]^{-1} \tag{2}$$

Here, T is the critical or cut-off angular momentum that is just grazing the nuclear surface and Δ is the rounding parameter. The parameter μ more accurately $\mu/4\Delta$ is a measure of real nuclear phase shift. A closed form expression for the elastic cross- section is then arrived at refs. [5, 6] in terms of three adjustable parameters, namely T, Δ and μ.The parameters T and Δ are related respectively to the interaction radius R and the surface diffuseness d through the relations

$$T = kR\left[1 - \frac{2n}{kR}\right]^{1/2} \tag{3}$$

$$\text{and} \quad \Delta = kd\left[1 - \frac{n}{kR}\right]\left[1 - \frac{2n}{kR}\right]^{1/2} \tag{4}$$

Where, n and k are respectively the Coulomb parameter and wave number.

The formalism developed for elastic scattering can be readily extended, under the condition for strong absorption, to describe inelastic scattering to collective states in nuclei. The inelastic scattering amplitude can be expressed in terms of the first derivative of scattering matrix η_ℓ used to describe the elastic scattering process.

It is clear from relations (1) and (2) that the real part of the scattering function η_ℓ varies smoothly with ℓ from small values at low ℓ's to unity at high ℓ's with a rapid transition around the critical values, while the imaginary part of η_ℓ is clearly surface peaked. A partial wave expression is made for the amplitude for elastic scattering and a closed form expression is obtained for the cross – section under suitable approximations.

3. Results and Discussion

3.1 Elastic Scattering

Results of the present analysis of elastic scattering are

Corresponding author: msuraju1971@yahoo.com

presented in Table 1 and the experimental data along with the theoretical calculated angular distributions are shown in Figs. 1-2. The data are taken from refs. [7-17]. A reasonably good description of the elastic scattering is possible in terms of the simple model. The observed oscillations in higher mass nuclei are also nicely matched over the entire angular range. The fit is generally poor at lower projectile energies. The quality of fit improves as we go higher up in energy. This is understandable, since the SAM conditions are strictly not satisfied in such light nucleus, more so at lower energies. The cut-off angular momentum T increases smoothly with an increase in beam energy, as expected. It is observed that rounding parameter Δ lies between 0.50- 5.10. The rounding parameter Δ increases with the increase in projectile energy. The parameter Δ controls the overall slope of the angular distribution and gives the periods of the diffraction of oscillation. The value of T and Δ are presented in Table 1. The value of nuclear phase shift μ or more accurately $\mu/4\Delta$ lies in the domain $0.07 \le \mu/4\Delta \le 0.40$ shown in Table 1.

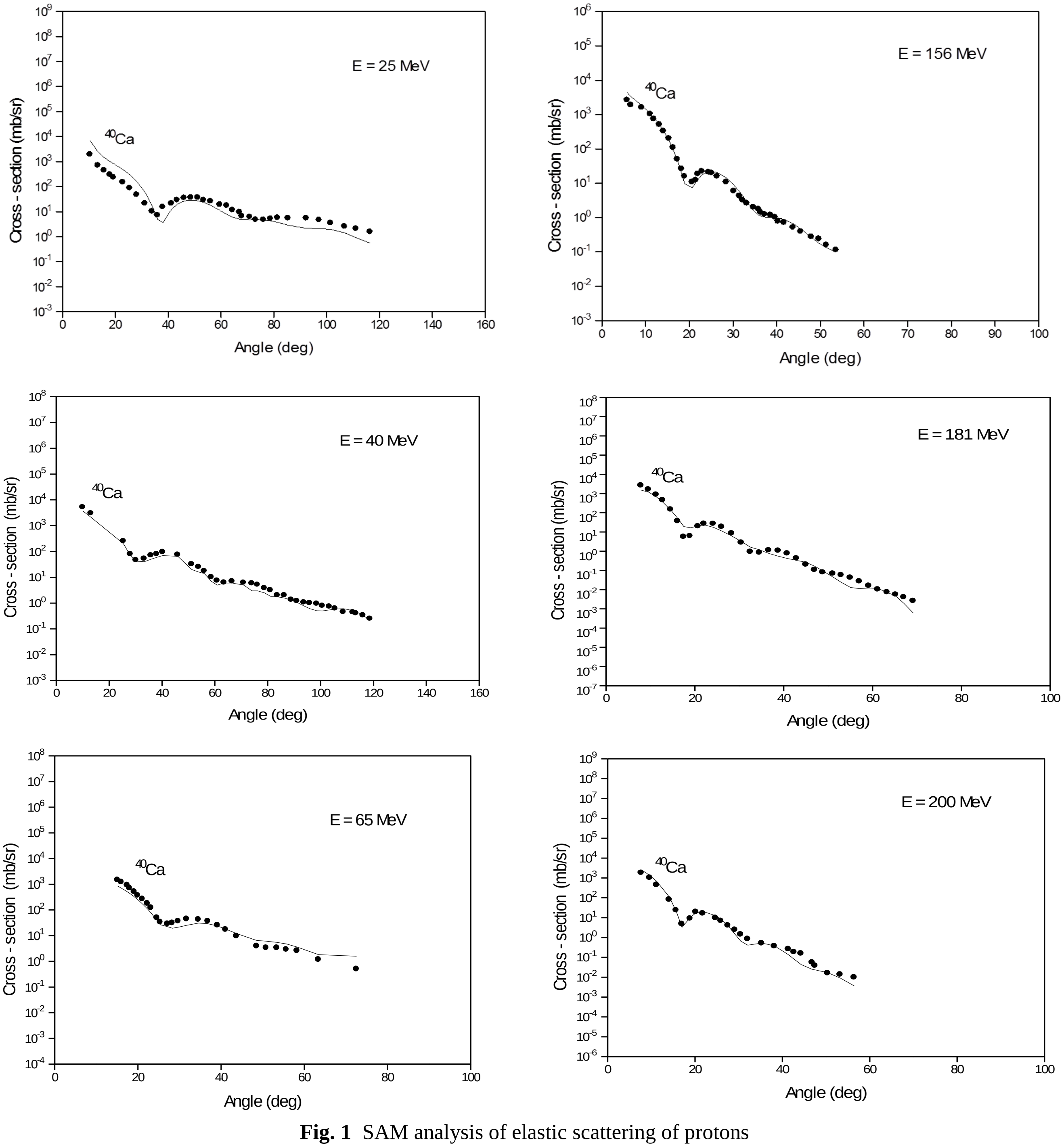

Fig. 1 SAM analysis of elastic scattering of protons

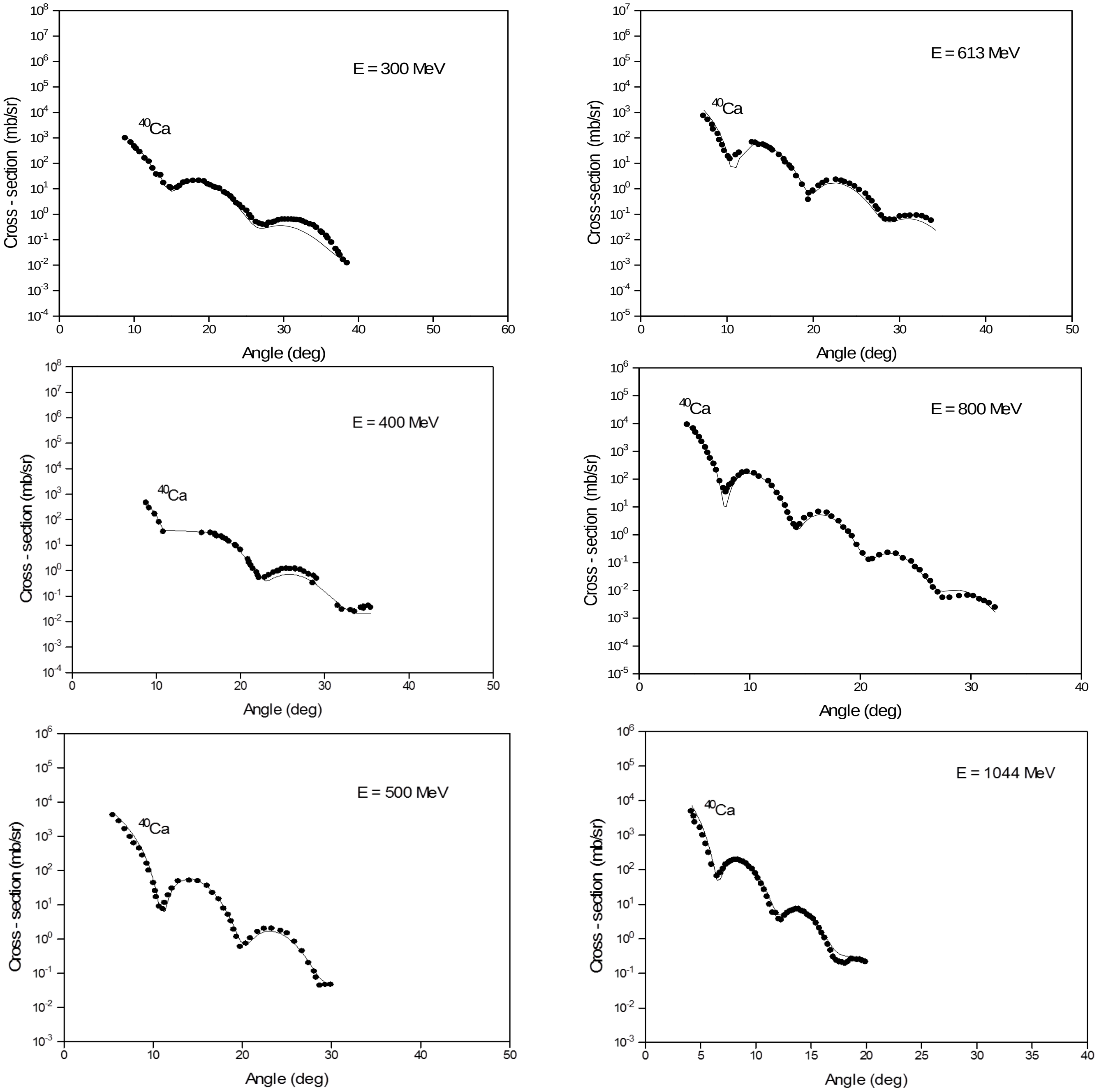

Fig. 2 SAM analysis of elastic scattering of protons

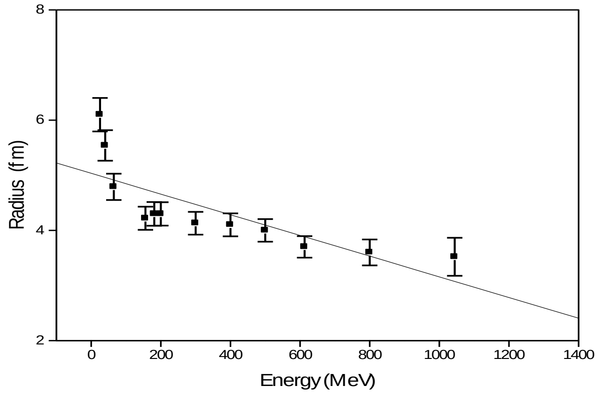

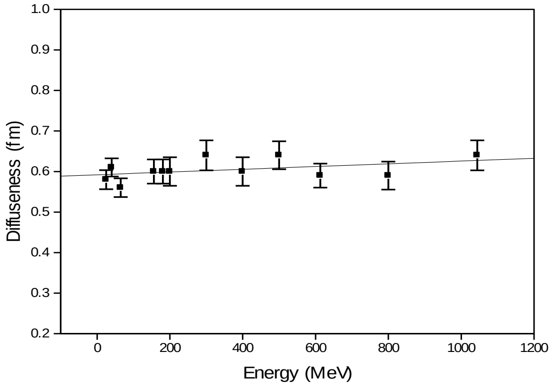

Fig. 3 Dependence of Radius (R) on proton energies

Fig. 4 Dependence of diffuseness (d) on Proton energies

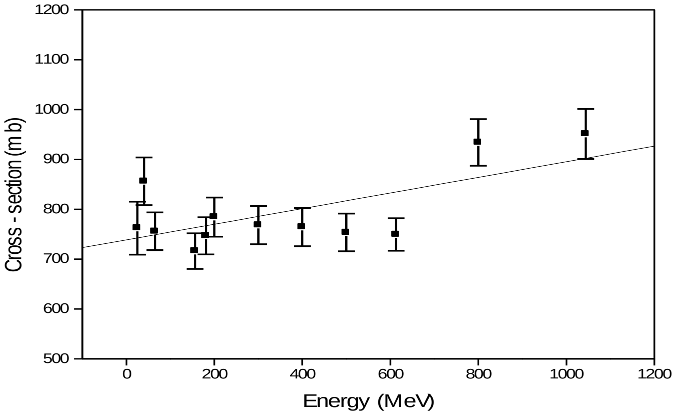

Fig. 5 Dependence of Cross section (σ_R) on proton energies

Table 1: SAM parameters and derived parameters for elastic scattering of protons

Serial No.	Target nucleus	Beam energy (MeV)	SAM parameters				Derived parameters						
			T	Δ	μ	μ/4Δ	R (fm)	d (fm)	θ_c (deg)	σ_R (mb)	r_o (fm)	$\frac{\sigma_R}{\pi R^2}$	n.v*
1	^{40}Ca	25	5.84	0.50	0.80	0.40	6.10	0.58	12.30	762.20	1.38	6.52	1
2	^{40}Ca	40	6.96	0.61	0.85	0.34	5.54	0.61	8.18	856.08	1.25	8.88	1.36
3	^{40}Ca	65	7.84	0.80	1.23	0.38	4.79	0.56	5.70	755.75	1.08	10.48	1.60
4	^{40}Ca	156	11.00	1.60	1.10	0.17	4.22	0.60	2.63	716.10	0.96	12.80	1.96
5	^{40}Ca	181	12.10	1.72	0.90	0.13	4.30	0.60	2.21	746.69	0.97	12.86	1.97
6	^{40}Ca	200	12.80	2.10	0.92	0.10	4.30	0.60	1.99	795.00	0.97	13.68	2.10
7	^{40}Ca	300	15.10	2.75	1.05	0.09	4.13	0.64	1.38	768.20	0.94	14.32	2.20
8	^{40}Ca	400	17.60	3.00	1.03	0.08	4.10	0.60	1.03	764.20	0.93	14.47	2.22
9	^{40}Ca	500	20.20	3.15	0.93	0.07	3.89	0.64	0.71	753.90	0.88	15.85	2.43
10	^{40}Ca	613	20.50	3.10	0.98	0.08	3.70	0.59	0.56	749.51	0.88	17.42	2.67
11	^{40}Ca	800	28.20	4.15	1.20	0.07	4.60	0.59	0.42	934.11	1.06	14.05	2.15
12	^{40}Ca	1044	33.20	5.10	2.25	0.11	5.89	0.64	0.34	950.90	1.09	8.72	1.34

Here, n.v* refers to the normalized value of $\frac{\sigma_R}{\pi R^2}$

The best fit SAM parameters are then used to determine the interaction radius R, the surface diffuseness d and the reaction cross-section σ_R. These are also shown in Table 1. It is evident from our studies that the value of R decreases as the beam energy increases for the same target nuclei shown in Fig. 3. The interaction radius R is sensibly constant as evidenced by the least squares fit given by

$$R = 5.03 - 0.0019E \text{ (fm)}$$

We see from the present study that the surface diffuseness d is approximately the same for different nuclei at all the energies shown in Fig. 4.

The energy dependence of reaction cross-section σ_R is shown in Fig.5. The least square fit given by

$$\sigma_R = 738.69 + 0.150E \text{ (mb)}$$

3.2 Inelastic scattering

The best fit parameters T, Δ and μ have been used to study the inelastic scattering of protons. The angular distribution data for the inelastic scattering of protons leading to a few collective states such as 2^+ and 3^- in ^{40}Ca have been analyzed in terms of the SAM formalism given by Potgieter and Frahn [16]. Fits to the inelastic angular distributions are shown in Figs. 6-7. The overall trend of the angular distributions is reproduced by the theory. Results of the inelastic scattering analyses are presented in Table 2. Also included the various obtained data in the previous studies. The β_2 and β_3 values from the various measurements are summarized respectively by Raman et al. [14] and Spear [15]. The present values are in good agreement with the previous values. It has been pointed out by Satchler [18] that the real test of the parameters obtained from the elastic scattering lies in their ability in reproducing the non-elastic data.

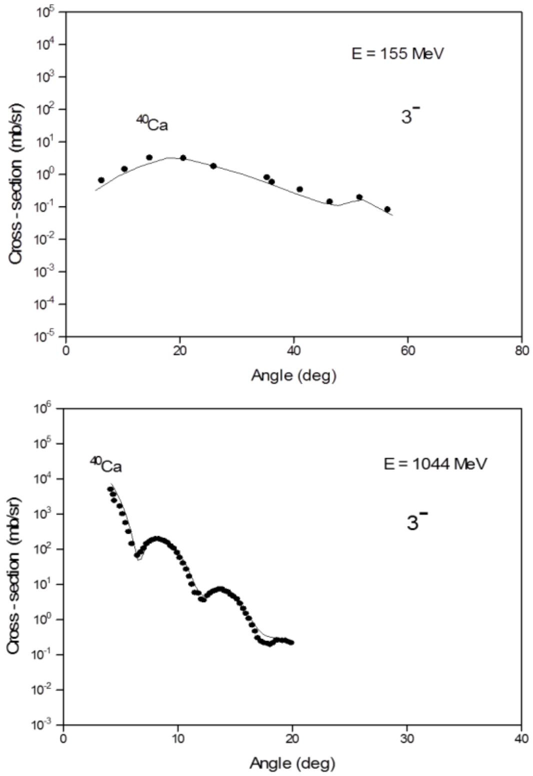

Fig. 6 SAM fit to the inelastic scattering of proton leading to the 3^{-} state

Table 2: Deformation parameters from inelastic scattering of protons leading to 2^{+} and 3^{-} states in nuclei

Nucleus	E_p (MeV)	E_x (MeV)	J^{π}	Deformation parameters β_L		
				a	b	C
^{40}Ca	500	3.904	2^{+}	0.447	0.49 – 0.50	
^{40}Ca	155	3.737	3^{-}	0.36		0.33 –0.36
^{40}Ca	1044	3.737	3^{-}	0.34		0.33 –0.36

a. Present work (SAM analyses), b. Previous work [14] c. Previous work [15]

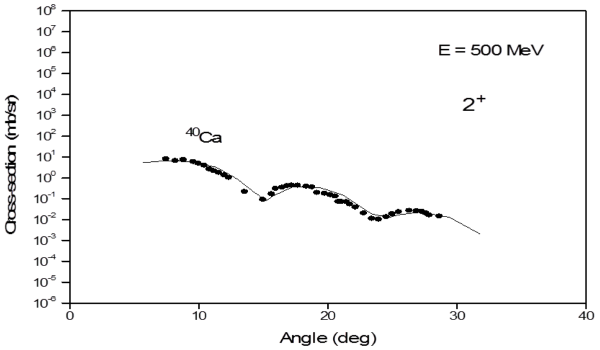

Fig. 7 SAM fit to the inelastic scattering of proton leading to the 2+ state

The β_2 and β_3 values from the various measurements are summarized respectively by Raman et al. [14] and Spear [15]. The present values are in good agreement with the previous values. It has been pointed out by Satchler [18] that the real test of the parameters obtained from the elastic scattering lies in their ability in reproducing the non-elastic data.

4. Conclusion

The three parameters (T, Δ, and μ) SAM formalism of Frahn and Venter [1, 2] can reasonably well account for the elastic scattering of protons. The angular distributions of the elastic scattering of protons from ^{40}Ca at 25 - 1044 MeV energies have been analyzed with SAM formalism and the best fit parameters T, Δ, and μ have been obtained. The quality of agreement between experiment and theory is much better for both the elastic and inelastic scattering using SAM formalism of Frahn and Venter. It is observed that the fittings of theoretical angular distribution are poor at low beam energies and smaller angels while at large energies the fittings become fairly improved. The values $\frac{\sigma_R}{\pi R^2}$ lie in the limit 0.4 ~ 1.0 and can be considered to be roughly the same, justifying the validity of the SAM parameters obtained from elastic scattering analyses. Another validation comes from the reasonable reproduction of the inelastic angular distribution and from quadrupole (β_2) and octupole (β_3) parameters values. The SAM is thus a successful model; the parameters are all unique and physically meaningful. The beauty of the model lies in its simplicity.

References

1. W. E. Frahn and R. H. Venter, Strong absorption model for elastic nuclear scattering part–I, Ann. Phys., (N.Y.), **24**, 243 (1963).
2. W. E. Frahn and R. H. Venter, Strong absorption model for elastic nuclear scattering and polarization of spin-12 particles, Ann. Phys., (N.Y.), **27**, 385 (1964).
3. K. R. Greider and Glassgold, Diffraction theory for very-high-energy scattering, Ann. Phys., **10**, 100 (1960).
4. J. A. McIntyre, K.W Wang and L. C. Beeker, Analysis of alpha-particle elastic scattering experiments, Phys. Rev., **A117,** 1337 (1960).
5. R. H. Venter, Strong absorption model for elastic nuclear scattering part –II, Ann. Phys., **25**, 405 (1963).
6. W. E. Frahn and B. Wiechers, Analysis of ^{3}He-nucleus scattering and polarization, Nucl. Phys., **74**, 65 (1965).
7. W. E. Frahn, Fundamentals in Nucl. Theory (IAEA), Vienna, **I** (1967).
8. L. F. Hansen, J. L. Kammerdiener and M. S. Weiss, Analysis of the scattering of 24-MeV ^{3}He particles from the even isotopes of zinc, Phys. Rev., **C4,** 1189 (1971).
9. N. Wills. I. Brissaud, Y. L. E. Bornec, B. Tatischeff and G. Duhames, Analysis of the (^{3}He, t) reaction on some 1p shell nuclei, Nucl. Phys., **A204**, 454 (1973).

10. M. Hyakutake, I. Kumabe, M. Fukuda, T. Komatuzaki, I. Yamagata, M. Inoue and H. Ogata, Elastic scattering of 119MeV He^3 particles and ^{15}N energy and mass number dependence of optical potential parameters, Nucl. Phys., A333, 1 (1980).
11. N. Matsuoka, K. Hatanaka, M. Fujiwara. Y. Fujita. T. Saito, K. Hosono, A. Shimizu and M. Kondo, DWBA analysis of (^3He, d) reactions at 90Mev and contributions from the nuclear interior, Nucl. Phys., **A373**, 377 (1982).
12. P. M. Lewis, A. K. Basak, J. D. Brown, P. V. Drumm, O. Karban, E.C. Pollacco and S. Roman, The elastic and inelastic scattering of 33Mev polarized ^3He from oxygen and iron isotope, Nucl. Phys., **A395,** 204 (1983).
13. S. Raman, C. H. Malarkey, W. T. Milner, C. W. J. Nestor and P. H. Steslon, Atomic data and nuclear data tables, **36**, 1 (1987).
14. M. A. Rahman, H. M. S. Gupta and M. Rahman, Strong absorption model for pion nucleus scattering around (3, 3) resonance, Phys. Rev., **C44**, 2484 (1991).
15. R. H. Spear, Atomic data and nuclear data tables, **42**, 55 (1989).
16. J. M. Potgietr and W. E. Frahn, Strong absorption model for inelastic nuclear scattering, Nucl. Phys., **80**, 434 (1967).
17. D. R. Sarker, H. Kabir, M. A Rahman and H. M. S. Gupta, Generalized diffraction model study of intermediate energy proton-nucleus scattering, Int. J. Mod. Phys., **E13(2),** 505 (2004).
18. G. R. Satchler, Proc. Int. Conf. Reactions between complex Nuclei, Nashville Tennessee (North-Holland Publishing Co., Amsterdam, 1974).